Artificial Sweeteners Induce Glucose Intolerance by Altering the Gut Microbiota

17 authors, including:

Jotham Suez
Weizmann Institute of Science
25 PUBLICATIONS   **1,134** CITATIONS

SEE PROFILE

Tal Korem
Weizmann Institute of Science
12 PUBLICATIONS   **1,214** CITATIONS

SEE PROFILE

David Zeevi
The Rockefeller University
18 PUBLICATIONS   **1,257** CITATIONS

SEE PROFILE

Ori Maza
Weizmann Institute of Science
1 PUBLICATION   **423** CITATIONS

SEE PROFILE

Some of the authors of this publication are also working on these related projects:

Project   Obesity and the Microbiome View project

Project   Analyzing the Mechanisms for the Assembly of Functional Mineral Scaffolds within Microbial Biofilms
View project

ARTICLE

Artificial sweeteners induce glucose intolerance by altering the gut microbiota

Jotham Suez[1], Tal Korem[2]*, David Zeevi[2]*, Gili Zilberman-Schapira[1]*, Christoph A. Thaiss[1], Ori Maza[1], David Israeli[3], Niv Zmora[4,5,6], Shlomit Gilad[7], Adina Weinberger[2], Yael Kuperman[8], Alon Harmelin[8], Ilana Kolodkin-Gal[9], Hagit Shapiro[1], Zamir Halpern[5,6], Eran Segal[2] & Eran Elinav[1]

Non-caloric artificial sweeteners (NAS) are among the most widely used food additives worldwide, regularly consumed by lean and obese individuals alike. NAS consumption is considered safe and beneficial owing to their low caloric content, yet supporting scientific data remain sparse and controversial. Here we demonstrate that consumption of commonly used NAS formulations drives the development of glucose intolerance through induction of compositional and functional alterations to the intestinal microbiota. These NAS-mediated deleterious metabolic effects are abrogated by antibiotic treatment, and are fully transferrable to germ-free mice upon faecal transplantation of microbiota configurations from NAS-consuming mice, or of microbiota anaerobically incubated in the presence of NAS. We identify NAS-altered microbial metabolic pathways that are linked to host susceptibility to metabolic disease, and demonstrate similar NAS-induced dysbiosis and glucose intolerance in healthy human subjects. Collectively, our results link NAS consumption, dysbiosis and metabolic abnormalities, thereby calling for a reassessment of massive NAS usage.

Non-caloric artificial sweeteners (NAS) were introduced over a century ago as means for providing sweet taste to foods without the associated high energy content of caloric sugars. NAS consumption gained much popularity owing to their reduced costs, low caloric intake and perceived health benefits for weight reduction and normalization of blood sugar levels[1]. For these reasons, NAS are increasingly introduced into commonly consumed foods such as diet sodas, cereals and sugar-free desserts, and are being recommended for weight loss and for individuals suffering from glucose intolerance and type 2 diabetes mellitus[1].

Some studies showed benefits for NAS consumption[2] and little induction of a glycaemic response[3], whereas others demonstrated associations between NAS consumption and weight gain[4], and increased type 2 diabetes risk[5]. However, interpretation is complicated by the fact that NAS are typically consumed by individuals already suffering from metabolic syndrome manifestations. Despite these controversial data, the US Food and Drug Administration (FDA) approved six NAS products for use in the United States.

Most NAS pass through the human gastrointestinal tract without being digested by the host[6,7] and thus directly encounter the intestinal microbiota, which plays central roles in regulating multiple physiological processes[8]. Microbiota composition[9] and function[10] are modulated by diet in the healthy/lean state as well as in obesity[11,12] and diabetes mellitus[13], and in turn microbiota alterations have been associated with propensity to metabolic syndrome[14]. Here, we study NAS-mediated modulation of microbiota composition and function, and the resultant effects on host glucose metabolism.

Chronic NAS consumption exacerbates glucose intolerance

To determine the effects of NAS on glucose homeostasis, we added commercial formulations of saccharin, sucralose or aspartame to the drinking water of lean 10-week-old C57Bl/6 mice (Extended Data Fig. 1a). Since all three commercial NAS comprise ~5% sweetener and ~95% glucose, we used as controls mice drinking only water or water supplemented with either glucose or sucrose. Notably, at week 11, the three mouse groups that consumed water, glucose and sucrose featured comparable glucose tolerance curves, whereas all three NAS-consuming mouse groups developed marked glucose intolerance ($P < 0.001$, Fig. 1a, b).

As saccharin exerted the most pronounced effect, we further studied its role as a prototypical artificial sweetener. To corroborate the findings in the obesity setup, we fed C57Bl/6 mice a high-fat diet (HFD, 60% kcal from fat) while consuming either commercial saccharin or pure glucose as a control (Extended Data Fig. 1b). As in the lean state, mice fed HFD and commercial saccharin developed glucose intolerance, compared to the control mouse group ($P < 0.03$, Fig. 1c and Extended Data Fig. 2a). To examine the effects of pure saccharin on glucose intolerance, we followed a cohort of 10-week-old C57Bl/6 mice fed on HFD and supplemented with 0.1 mg ml^{-1} of pure saccharin added to their drinking water (Extended Data Fig. 1c). This dose corresponds to the FDA acceptable daily intake (ADI) in humans (5 mg per kg (body weight), adjusted to mouse weights, see Methods). As with commercial saccharin, this lower dose of pure saccharin was associated with impaired glucose tolerance ($P < 0.0002$, Fig. 1d and Extended Data Fig. 2b) starting as early as 5 weeks after HFD initiation. Similarly, HFD-fed outbred Swiss Webster mice supplemented with or without 0.1 mg ml^{-1} of pure saccharin (Extended Data Fig. 1d) showed significant glucose intolerance after 5 weeks of saccharin exposure as compared to controls ($P < 0.03$, Extended Data Fig. 2c, d).

Metabolic profiling of normal-chow- or HFD-fed mice in metabolic cages, including liquids and chow consumption, oxygen consumption, walking distance and energy expenditure, showed similar measures between NAS- and control-drinking mice (Extended Data Fig. 3 and 4).
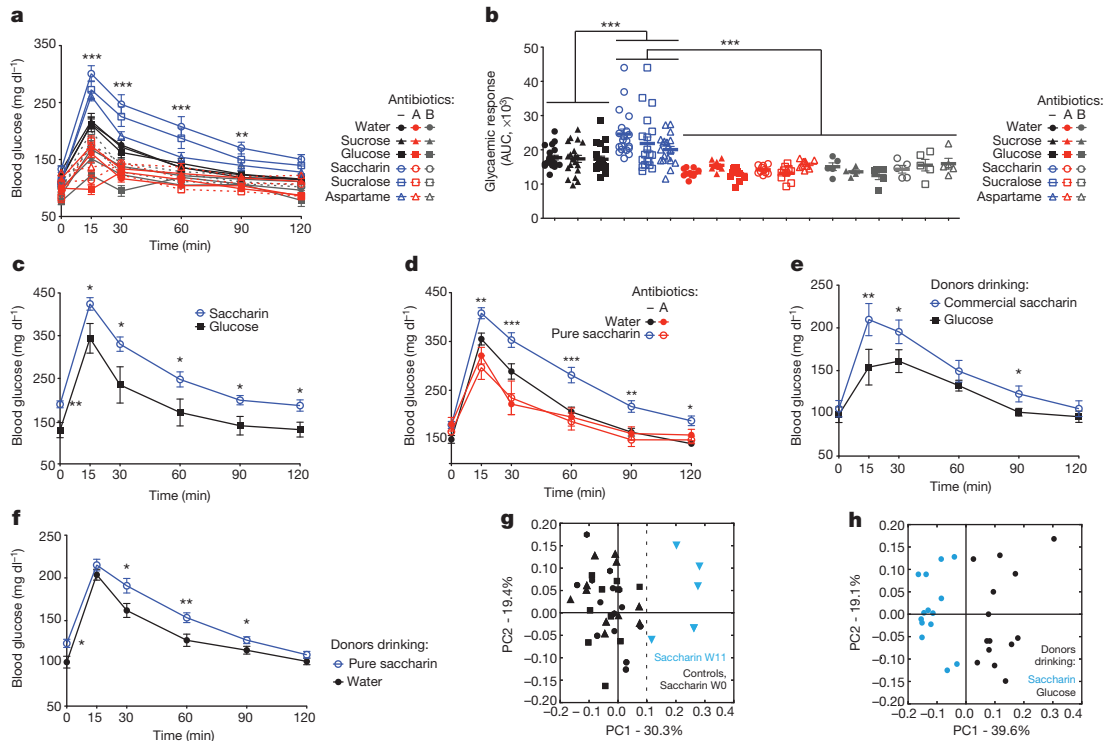
Figure 1 | Artificial sweeteners induce glucose intolerance transferable to germ-free mice. a, b, Oral glucose tolerance test (OGTT, **a**) and area under the two-hour blood glucose response curve (AUC, **b**) in normal-chow-fed mice drinking commercial NAS for 11 weeks before ($N = 20$) and after antibiotics: ciprofloxacin and metronidazole ('antibiotics A', $N = 10$); or vancomycin ('antibiotics B', $N = 5$). **c**, OGTT in mice fed HFD and commercial saccharin ($N = 10$) or glucose ($N = 9$). **d**, OGTT of HFD-fed mice drinking 0.1 mg ml^{-1} saccharin or water for 5 weeks ($N = 20$), followed by 'antibiotics A' ($N = 10$). **e, f**, OGTT of germ-free mice 6 days following transplant of microbiota from commercial saccharin- ($N = 12$) and glucose-fed mice ($N = 11$) (**e**), or pure

saccharin- ($N = 16$) and water-fed ($N = 16$) donors (**f**). Symbols (OGTT) or horizontal lines (AUC), mean; error bars, s.e.m. *$P < 0.05$, **$P < 0.01$, ***$P < 0.001$. OGTT, analysis of variance (ANOVA) and Bonferroni; AUC, ANOVA and Tukey post hoc analysis. Each experiment was repeated twice. **g**, Principal coordinates analysis (PCoA) of weighted UniFrac distances based on 16S rRNA analysis from saccharin-consuming mice at baseline (W0, black hexagons; W11, blue triangles); water controls (black circles for W11 and W0); glucose (black squares for W11 and W0); or sucrose (black triangles for W11 and W0). $N = 5$ in each group. **h**, PCoA of taxa in germ-free recipients according to donor identity in **e**.

Fasting serum insulin levels and insulin tolerance were also similar in all mouse groups consuming NAS or caloric sweeteners, in both the normal-chow and HFD settings (Extended Data Fig. 5). Taken together, these results suggest that NAS promote metabolic derangements in a range of formulations, doses, mouse strains and diets paralleling human conditions, in both the lean and the obese state.

Gut microbiota mediates NAS–induced glucose intolerance

Since diet modulates the gut microbiota[15], and microbiota alterations exert profound effects on host physiology and metabolism, we tested whether the microbiota may regulate the observed NAS effects. To this end, we treated mouse groups consuming commercial or pure NAS in the lean and HFD states (Extended Data Fig. 1a, c) with a Gram-negative-targeting broad-spectrum antibiotics regimen (designated 'antibiotics A') of ciprofloxacin (0.2 g l^{-1}) and metronidazole (1 g l^{-1}), while maintaining mice on their diet and sweetener supplementation regimens. Notably, after 4 weeks of antibiotic treatment, differences in glucose intolerance between NAS-drinking mice and controls were abolished both in the lean (Fig. 1a, b) and the obese (Fig. 1d and Extended Data Fig. 2b) states. Similar effects were observed with the Gram-positive-targeting antibiotic vancomycin ('antibiotics B', 0.5 g l^{-1}, Fig. 1a, b). These results suggest that NAS-induced glucose intolerance is mediated through alterations to the commensal microbiota, with contributions from diverse bacterial taxa.

To test whether the microbiota role is causal, we performed faecal transplantation experiments, by transferring the microbiota configuration from mice on normal-chow diet drinking commercial saccharin

or glucose (control) into normal-chow-consuming germ-free mice (Extended Data Fig. 1e). Notably, recipients of microbiota from mice consuming commercial saccharin exhibited impaired glucose tolerance as compared to control (glucose) microbiota recipients, determined 6 days following transfer ($P < 0.03$, Fig. 1e and Extended Data Fig. 2e). Transferring the microbiota composition of HFD-consuming mice drinking water or pure saccharin replicated the glucose intolerance phenotype ($P < 0.004$, Fig. 1f and Extended Data Fig. 2f). Together, these results establish that the metabolic derangements induced by NAS consumption are mediated by the intestinal microbiota.

NAS mediate distinct functional alterations to the microbiota

We next examined the faecal microbiota composition of our various mouse groups by sequencing their 16S ribosomal RNA gene. Mice drinking saccharin had a distinct microbiota composition that clustered separately from both their starting microbiome configurations and from all control groups at week 11 (Fig. 1g). Likewise, microbiota in germ-free recipients of stools from saccharin-consuming donor mice clustered separately from that of germ-free recipients of glucose-drinking donor stools (Fig. 1h). Compared to all control groups, the microbiota of saccharin-consuming mice displayed considerable dysbiosis, with more than 40 operational taxonomic units (OTUs) significantly altered in abundance (false discovery rate (FDR) corrected P value < 0.05 for each OTU; Extended Data Fig. 6, Supplementary Table 1). Many of the taxa that increased in relative abundance belonged to the *Bacteroides* genus and Clostridiales order, with other members of the Clostridiales order comprising the majority of under-represented taxa, along with *Lactobacillus reuteri*, and were

mirrored in germ-free recipients of stools from saccharin-consuming donors (Extended Data Fig. 6, right column). Likewise, dysbiosis was observed in mice consuming pure saccharin and HFD (Supplementary Table 1). Together, these results demonstrate that saccharin consumption in various formulations, doses and diets induces dysbiosis with overall similar configurations.

To study the functional consequences of NAS consumption, we performed shotgun metagenomic sequencing of faecal samples from before and after 11 weeks of commercial saccharin consumption, compared to control mice consuming either glucose or water. To compare relative species abundance, we mapped sequencing reads to the human microbiome project reference genome database[16]. In agreement with the 16S rRNA analysis, saccharin treatment induced the largest changes in microbial relative species abundance (Fig. 2a, Supplementary Table 2; F-test P value $< 10^{-10}$). These changes are unlikely to be an artefact of horizontal gene transfer or poorly covered genomes, because changes in relative abundance were observed across much of the length of the bacterial genomes, as exemplified by one overrepresented (*Bacteroides vulgatus*, Extended Data Fig. 7a) and one underrepresented species (*Akkermansia muciniphila*, Extended Data Fig. 7b).

We next mapped the metagenomic reads to a gut microbial gene catalogue, evenly dividing reads mapping to more than one gene, and then grouping genes into KEGG (Kyoto Encyclopedia of Genes and Genomes) pathways. Examining pathways with gene coverage above 0.2 (115 pathways), changes in pathway abundance were inversely correlated between commercial saccharin- and glucose-consuming mice ($R = -0.45$, $P < 10^{-6}$, Fig. 2b). Since commercial saccharin consists of 95% glucose, these results suggest that saccharin greatly affects microbiota function. Notably, pathways overrepresented in saccharin-consuming mice include a strong increase in glycan degradation pathways (Fig. 2c, d), in which glycans are fermented to form various compounds including short-chain fatty acids (SCFAs)[17]. These pathways mark enhanced energy harvest and their enrichment was previously associated with obesity in mice[11] and humans[18], with SCFA possibly serving as precursors and/or signalling molecules for *de novo* glucose and lipid synthesis by the host[19]. To identify the underlying bacteria, we annotated every read that mapped to glycan degradation pathways by its originating bacteria. Much of the increase in these pathways is attributable to reads originating from five Gram-negative and -positive species, of which two belong to the

Bacteroides genus (Fig. 2e). This is consistent with the sharp increase in the abundance of this genus in saccharin-consuming mice observed in the 16S rRNA analysis (Extended Data Fig. 6). Consequently, levels of the SCFAs propionate and acetate measured in stool were markedly higher in commercial saccharin-consuming mice compared to control glucose-consuming mice (Fig. 2f, g), reflective of the differential effects mediated by chronic glucose consumption with and without NAS exposure. Butyrate levels were similar between the groups (data not shown).

In addition to glycan degradation, and similar to previous studies on humans with type 2 diabetes[13,20], other pathways were enriched in microbiomes of saccharin-consuming mice, including starch and sucrose metabolism, fructose and mannose metabolism, and folate, glycerolipid and fatty acid biosynthesis (Supplementary Tables 3 and 4), whereas glucose transport pathways were underrepresented in saccharin-consuming mice (Extended Data Fig. 7c). Mice consuming HFD and pure saccharin featured several enriched pathways (Extended Data Fig. 7d), including ascorbate and aldarate metabolism (previously reported to be enriched in leptin-receptor-deficient diabetic mice[21]), lipopolysaccharide biosynthesis (linked to metabolic endotoxemia[22]) and bacterial chemotaxis (previously reported to be enriched in obese mice[11]).

Altogether, saccharin consumption results in distinct diet-dependent functional alterations in the microbiota, including normal-chow-related expansion in glycan degradation contributed by several of the increased taxa, ultimately resulting in elevated stool SCFA levels, characteristic of increased microbial energy harvest[11].

NAS directly modulate the microbiota to induce glucose intolerance

To determine whether saccharin directly affects the gut microbiota, we cultured faecal matter from naive mice under strict anaerobic conditions (75% N_2, 20% CO_2, 5% H_2) in the presence of saccharin (5 mg ml^{-1}) or control growth media. Cultures from day 9 of incubation were administered by gavage to germ-free mice (Extended Data Fig. 8a). *In vitro* stool culture with saccharin induced an increase of the Bacteroidetes phylum and reduction in Firmicutes (Bacteroidetes 89% versus 70%, Firmicutes 6% versus 22%, Extended Data Fig. 8b). Transferring this *in vitro* saccharin-treated microbiota configuration into germ-free mice resulted in significantly higher glucose intolerance ($P < 0.002$) compared with germ-free mice receiving the control culture (Fig. 3a and Extended
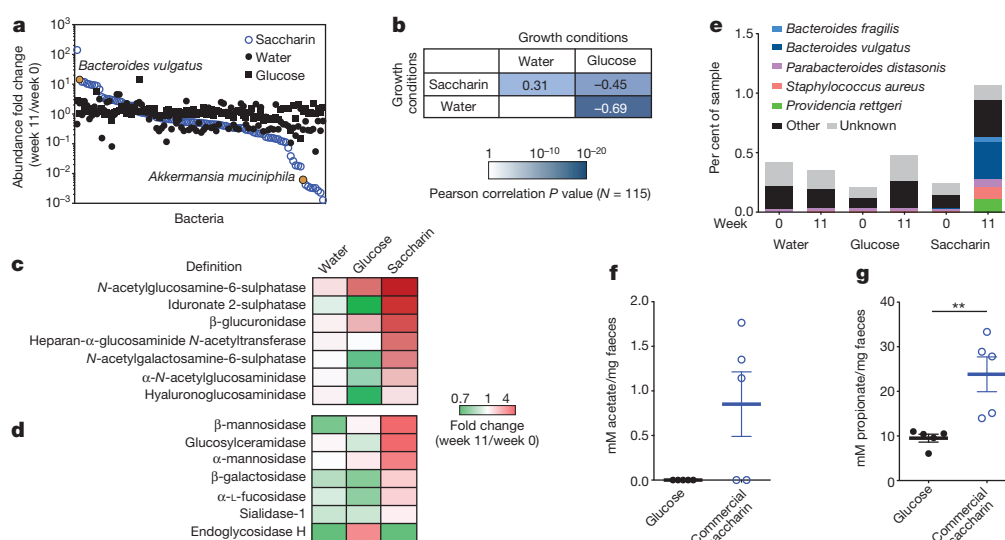

Figure 2 | Functional characterization of saccharin-modulated microbiota. a, Species alterations in mice consuming commercial saccharin, water or glucose for 11 weeks ($N = 4$) shown by shotgun sequencing. **b**, Pairwise correlations between changes in 115 KEGG pathways across mice receiving different treatments. **c, d**, Fold change in relative abundance of glycosaminoglycan (**c**) or other glycan (**d**) degradation pathway genes.

e, Higher glycan degradation attributed to five taxa in the commercial saccharin setting. **f, g**, Levels of faecal acetate and propionate at W11 in mice drinking commercial saccharin or glucose ($N = 5$). Horizontal lines, means; error bars, s.e.m. **$P < 0.01$, two-sided unpaired Student *t*-test. SCFA measurements were performed on two independent cohorts.

Data Fig. 8c). Similar to the composition of the saccharin-supplemented anaerobic culture, germ-free recipients of this cultured configuration featured over-representation of members of the *Bacteroides* genus, and under-representation of several Clostridiales (Fig. 3b and Supplementary Table 5).

Shotgun metagenomic sequencing analysis revealed that *in vitro* saccharin treatment induced similar functional alterations to those found in mice consuming commercial saccharin (Fig. 4c, $P < 10^{-4}$), with glycan degradation pathways being highly enriched in both settings. Other pathways highly enriched in both settings included those involved in sphingolipid metabolism, previously shown to be over-represented in microbiomes of non-obese diabetic mice[23], and common under-represented pathways included glucose transport (Fig. 3c and Extended Data 7c, right column).

Collectively, these results demonstrate that saccharin directly modulates the composition and function of the microbiome and induces
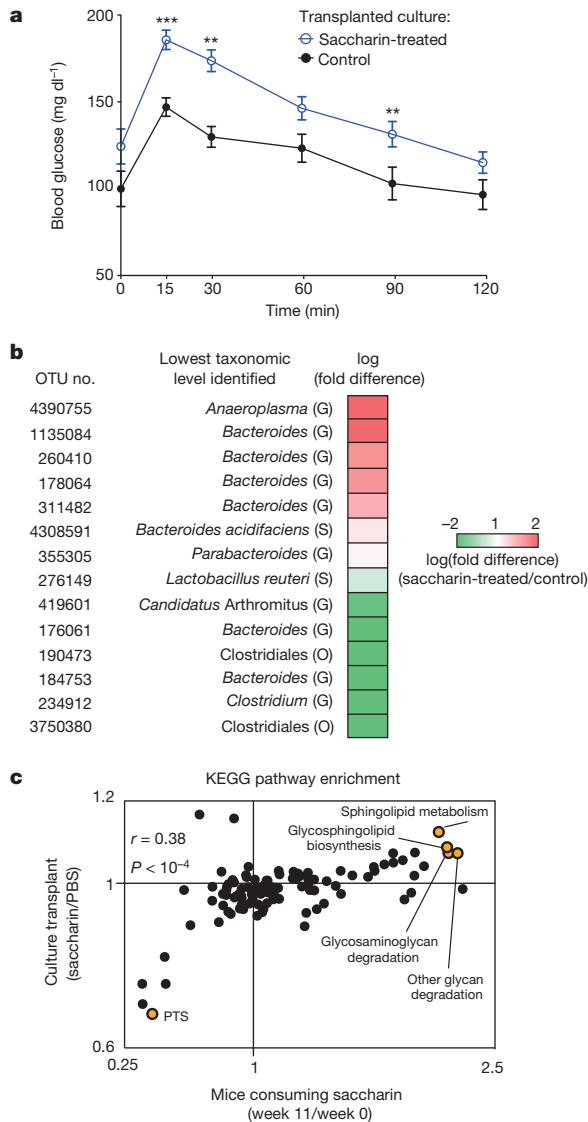

Figure 3 | Saccharin directly modulates the microbiota. a, OGTT of germ-free mice 6 days following transplantation with saccharin-enriched or control faecal cultures ($N = 10$ and $N = 9$, respectively). Symbols, means; error bars, s.e.m. **$P < 0.01$, ***$P < 0.001$, ANOVA and Bonferroni post hoc analysis. Experiments were repeated twice. **b**, Taxa representation in germ-free mice from **a**. O, order; G, genus; S, species. **c**, Comparison of KEGG pathway abundance between W11 saccharin-consuming mice (compared to W0, *x* axis) and germ-free mice transplanted with microbiomes anaerobically cultured with 5 mg ml^{-1} saccharin (compared to PBS, *y* axis).
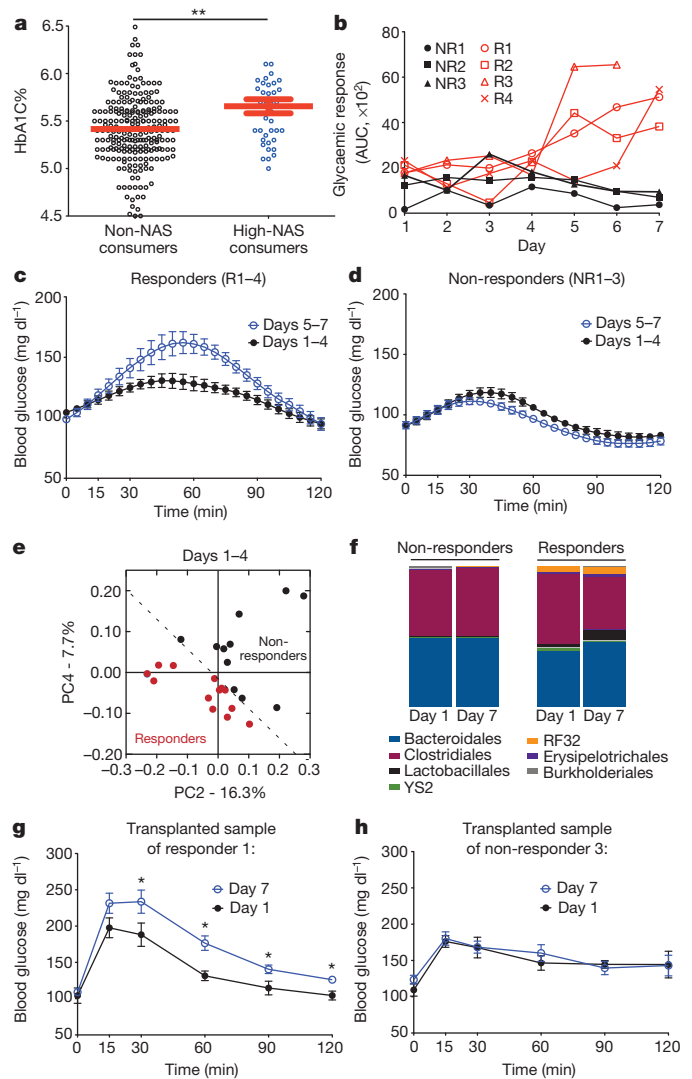

Figure 4 | Acute saccharin consumption impairs glycaemic control in humans by inducing dysbiosis. a, HbA1C% of high NAS consumers ($N = 40$) versus non-consumers ($N = 236$). **Rank sum *P* value < 0.002. **b**, Daily incremental area under the curve (iAUC) of OGTT in 4 responders (R) and 3 non-responders (NR). **c, d**, OGTT of days 1–4 versus days 5–7 in 4 responders (**c**) or 3 non-responders (**d**). **e**, PCoA of 16S rRNA sequences from responders (N samples = 16) versus non-responders (N = 9) during days 1–4. **f**, Order-level relative abundance of taxa samples from days 1 and 7 of responders and non-responders. **g, h**, OGTT in germ-free mice ($N = 6$) 6 days following faecal transplantation of D1 or D7 samples of responder 1 (R1, **g**) or non-responder 3 (NR3, **h**). Symbols, means; error bars, s.e.m. *$P < 0.05$, **$P < 0.01$, ANOVA and Bonferroni post hoc analysis.

dysbiosis, accounting for the downstream glucose intolerance phenotype in the mammalian host.

NAS in humans associate with impaired glucose tolerance

To study the effect of NAS in humans, we examined the relationship between long-term NAS consumption (based on a validated food frequency questionnaire, see Methods) and various clinical parameters in data collected from 381 non-diabetic individuals (44% males and 56% females; age 43.3 ± 13.2) in an ongoing clinical nutritional study. We found significant positive correlations between NAS consumption and several metabolic-syndrome-related clinical parameters (Supplementary Table 6), including increased weight and waist-to-hip ratio (measures of central obesity); higher fasting blood glucose, glycosylated

haemoglobin (HbA1C%) and glucose tolerance test (GTT, measures of impaired glucose tolerance), and elevated serum alanine aminotransferase (ALT, measure of hepatic damage that is likely to be secondary, in this context, to non-alcoholic fatty liver disease). Moreover, the levels of glycosylated haemoglobin (HbA1C%), indicative of glucose concentration over the previous 3 months, were significantly increased when comparing a subgroup of high NAS consumers (40 individuals) to non-NAS consumers (236 individuals, Fig. 4a, rank sum $P < 0.002$). This increase remained significant when corrected to body mass index (BMI) levels (rank sum $P < 0.015$). In this cohort, we characterized the 16S rRNA in 172 randomly selected individuals. Notably, we found statistically significant positive correlations between multiple taxonomic entities and NAS consumption, including the *Enterobacteriaceae* family (Pearson $r = 0.36$, FDR corrected $P < 10^{-6}$), the Deltaproteobacteria class (Pearson $r = 0.33$, FDR corrected $P < 10^{-5}$) and the Actinobacteria phylum (Pearson $r = 0.27$, FDR corrected $P < 0.0003$, Supplementary Table 7). Importantly, we did not detect statistically significant correlations between OTU abundances and BMI, suggesting that the above correlations are not due to the distinct BMI of NAS consumers.

Finally, as an initial assessment of whether the relationship between human NAS consumption and blood glucose control is causative, we followed seven healthy volunteers (5 males and 2 females, aged 28–36) who do not normally consume NAS or NAS-containing foods for 1 week. During this week, participants consumed on days 2–7 the FDA's maximal acceptable daily intake (ADI) of commercial saccharin (5 mg per kg (body weight)) as three divided daily doses equivalent to 120 mg, and were monitored by continuous glucose measurements and daily GTT (Extended Data Fig. 9a). Notably, even in this short-term 7-day exposure period, most individuals (4 out of 7) developed significantly poorer glycaemic responses 5–7 days after NAS consumption (hereafter termed 'NAS responders'), compared to their individual glycaemic response on days 1–4 (Fig. 4b, c and Extended Data Fig. 9b, $P < 0.001$). None of the three NAS non-responders featured improved glucose tolerance (Fig. 4b, d and Extended Data Fig. 9c).

The microbiome configurations of NAS responders, as assessed by 16S rRNA analysis, clustered differently from non-responders both before and after NAS consumption (Fig. 4e and Extended Data Fig. 9d, respectively). Moreover, microbiomes from non-responders featured little changes in composition during the study week, whereas pronounced compositional changes were observed in NAS responders (Fig. 4f and Extended Data Fig. 9e). To study whether this NAS-induced dysbiosis has a causal role in generating glucose intolerance, stool from before (day 1, D1) or after (day 7, D7) NAS exposure were transferred from two NAS responders and two NAS non-responders into groups of normal-chow-fed germ-free mice. Indeed, transfer of post-NAS exposure (D7) stool from NAS responders induced significant glucose intolerance in recipient germ-free mice, compared to the response noted with D1 stool transferred from the same NAS-responding individuals (Fig. 4g and Extended Data Fig. 9f, $P < 0.004$ and Extended Data 9g, h, $P < 0.02$). In contrast, D7 stools transferred into germ-free mice from the two NAS non-responders induced normal glucose tolerance, which was indistinguishable from that of mice transferred with D1 stools from the same 'non-responding' individuals (Fig. 4h and Extended Data Fig. 9i–k). Germ-free mice transplanted with 'responders' microbiome replicated some of the donor saccharin-induced dysbiosis, including 20-fold relative increase of *Bacteroides fragilis* (order Bacteroidales) and *Weissella cibaria* (order Lactobacillales), and approximately tenfold decrease in *Candidatus* Arthromitus (order Clostridiales) (Extended Data Fig. 9l).

Discussion

In summary, our results suggest that NAS consumption in both mice and humans enhances the risk of glucose intolerance and that these adverse metabolic effects are mediated by modulation of the composition and function of the microbiota. Notably, several of the bacterial taxa that changed following NAS consumption were previously associated with type 2 diabetes in humans[13,20], including over-representation

of *Bacteroides* and under-representation of Clostridiales. Both Gram-positive and Gram-negative taxa contributed to the NAS-induced phenotype (Fig. 1a, b) and were enriched for glycan degradation pathways (Extended Data Fig. 6), previously linked to enhanced energy harvest (Fig. 2c, d)[11,24]. This suggests that elaborate inter-species microbial cooperation may functionally orchestrate the gut ecosystem and contribute to vital community activities in diverging environmental conditions (for example, normal-chow versus high-fat dietary conditions). In addition, we show that metagenomes of saccharin-consuming mice are enriched with multiple additional pathways previously shown to associate with diabetes mellitus[23] or obesity[11] in mice and humans, including sphingolipid metabolism and lipopolysaccharide biosynthesis[25].

Our results from short- and long-term human NAS consumer cohorts (Fig. 4, Extended Data Fig. 9 and Supplementary Tables 6, 7) suggest that human individuals feature a personalized response to NAS, possibly stemming from differences in their microbiota composition and function. The changes noted in our studies may be further substantiated in mice consuming different human diets[26]. Similarly, we believe that other individualized nutritional responses may be driven by personalized functional differences in the microbiome. As such, 'personalized nutrition' leading to 'personalized medical outcome' may underlie the variable nutritional effects noted in many multi-factorial diseases, and warrants further studies.

Artificial sweeteners were extensively introduced into our diets with the intention of reducing caloric intake and normalizing blood glucose levels without compromising the human 'sweet tooth'. Together with other major shifts that occurred in human nutrition, this increase in NAS consumption coincides with the dramatic increase in the obesity and diabetes epidemics. Our findings suggest that NAS may have directly contributed to enhancing the exact epidemic that they themselves were intended to fight. Moreover, our results point towards the need to develop new nutritional strategies tailored to the individual while integrating personalized differences in the composition and function of the gut microbiota.

Online Content Methods, along with any additional Extended Data display items and Source Data, are available in the online version of the paper; references unique to these sections appear only in the online paper.

1. Gardner, C. et al. Nonnutritive sweeteners: current use and health perspectives. *Diabetes Care* **35**, 1798–1808 (2012).
2. Fitch, C. & Keim, K. S. Position of the Academy of Nutrition and Dietetics: use of nutritive and nonnutritive sweeteners. *Journal of the Academy of Nutrition and Dietetics* **112**, 739–758 (2012).
3. Tordoff, M. G. & Alleva, A. M. Effect of drinking soda sweetened with aspartame or high-fructose corn syrup on food intake and body weight. *Am. J. Clin. Nutr.* **51**, 963–969 (1990).
4. Horwitz, D. L., McLane, M. & Kobe, P. Response to single dose of aspartame or saccharin by NIDDM patients. *Diabetes Care* **11**, 230–234 (1988).
5. Nettleton, J. A. et al. Diet soda intake and risk of incident metabolic syndrome and type 2 diabetes in the Multi-Ethnic Study of Atherosclerosis (MESA). *Diabetes Care* **32**, 688–694 (2009).
6. Roberts, A., Renwick, A. G., Sims, J. & Snodin, D. J. Sucralose metabolism and pharmacokinetics in man. *Food Chem. Toxicol.* **38** (Suppl. 2), 31–41 (2000).
7. Byard, J. L. & Goldberg, L. The metabolism of saccharin in laboratory animals. *Food Cosmet. Toxicol.* **11**, 391–402 (1973).
8. Clemente, J. C., Ursell, L. K., Parfrey, L. W. & Knight, R. The impact of the gut microbiota on human health: an integrative view. *Cell* **148**, 1258–1270 (2012).
9. Claesson, M. J. et al. Gut microbiota composition correlates with diet and health in the elderly. *Nature* **488**, 178–184 (2012).
10. Muegge, B. D. et al. Diet drives convergence in gut microbiome functions across mammalian phylogeny and within humans. *Science* **332**, 970–974 (2011).
11. Turnbaugh, P. J. et al. An obesity-associated gut microbiome with increased capacity for energy harvest. *Nature* **444**, 1027–1031 (2006).
12. Ley, R. E., Turnbaugh, P. J., Klein, S. & Gordon, J. I. Microbial ecology: human gut microbes associated with obesity. *Nature* **444**, 1022–1023 (2006).
13. Qin, J. et al. A metagenome-wide association study of gut microbiota in type 2 diabetes. *Nature* **490**, 55–60 (2012).
14. Henao-Mejia, J. et al. Inflammasome-mediated dysbiosis regulates progression of NAFLD and obesity. *Nature* **482**, 179–185 (2012).
15. David, L. A. et al. Diet rapidly and reproducibly alters the human gut microbiome. *Nature* **505**, 559–563 (2014).

16. Peterson, J. *et al*. The NIH human microbiome project. *Genome Res.* **19,** 2317–2323 (2009).
17. Koropatkin, N. M., Cameron, E. A. & Martens, E. C. How glycan metabolism shapes the human gut microbiota. *Nature Rev. Microbiol.* **10,** 323–335 (2012).
18. Schwiertz, A. *et al*. Microbiota and SCFA in lean and overweight healthy subjects. *Obesity* **18,** 190–195 (2010).
19. Bergman, E. N. Energy contributions of volatile fatty acids from the gastrointestinal tract in various species. *Physiol. Rev.* **70,** 567–590 (1990).
20. Karlsson, F. H. *et al*. Gut metagenome in European women with normal, impaired and diabetic glucose control. *Nature* **498,** 99–103 (2013).
21. Connor, S. C., Hansen, M. K., Corner, A., Smith, R. F. & Ryan, T. E. Integration of metabolomics and transcriptomics data to aid biomarker discovery in type 2 diabetes. *Mol. Biosyst.* **6,** 909–921 (2010).
22. Cani, P. D. *et al*. Changes in gut microbiota control metabolic endotoxemia-induced inflammation in high-fat diet-induced obesity and diabetes in mice. *Diabetes* **57,** 1470–1481 (2008).
23. Markle, J. G. *et al*. Sex differences in the gut microbiome drive hormone-dependent regulation of autoimmunity. *Science* **339,** 1084–1088 (2013).
24. Sonnenburg, J. L. *et al*. Glycan foraging *in vivo* by an intestine-adapted bacterial symbiont. *Science* **307,** 1955–1959 (2005).
25. Cani, P. D. *et al*. Metabolic endotoxemia initiates obesity and insulin resistance. *Diabetes* **56,** 1761–1772 (2007).
26. Smith, M. I. *et al*. Gut microbiomes of Malawian twin pairs discordant for kwashiorkor. *Science* **339,** 548–554 (2013).

Supplementary Information is available in the online version of the paper.

Author Contributions J.S. conceived the project, designed and performed experiments, interpreted the results, and wrote the manuscript. T.K., D.Z. and G.Z.-S. performed the computational and metagenomic microbiota analysis and the analysis of the retrospective and prospective human study, and are listed alphabetically. C.A.T., O.M., A.W. and H.S. helped with experiments. Y.K. helped with the metabolic cage experiments. S.G. designed the metagenomic library protocols and generated the libraries. I.K.-G. performed the SCFA quantification experiments. D.I., N.Z., and Z.H. performed and supervised human experimentation. A.H. supervised the germ-free mouse experiments. E.S. and E.E. conceived and directed the project, designed experiments, interpreted the results, and wrote the manuscript.

Author Information Sequencing data are deposited in the European Nucleotide Archive accession PRJEB6996. Reprints and permissions information is available at www.nature.com/reprints. The authors declare no competing financial interests. Readers are welcome to comment on the online version of the paper. Correspondence and requests for materials should be addressed to E.S. (eran.segal@weizmann.ac.il) or E.E. (eran.elinav@weizmann.ac.il).

METHODS

Mice. C57Bl/6 WT adult male mice were randomly assigned (without blinding) to treatment groups and were given commercial artificial sweeteners (saccharin-, sucralose- or aspartame-based) or pure saccharin (Sigma Aldrich) in drinking water and fed a high-fat (HFD D12492, 60% kcal from fat, Research Diets) or standard polysaccharide normal-chow diet (Harlan-Teklad). Compared groups were always fed from the same batch of diet. For antibiotic treatment, mice were given a combination of ciprofloxacin ($0.2\,g\,l^{-1}$) and metronidazole ($1\,g\,l^{-1}$) or vancomycin ($0.5\,g\,l^{-1}$) in their drinking water. All antibiotics were obtained from Sigma Aldrich. Adult male outbred Swiss-Webster mice (a widely used mouse strain in germ-free experiments) served as recipients for faecal transplants and were housed in sterile isolators (Park Bioservices). For faecal transplantation experiments, 200 mg of stool (from mouse pellets or human swabs) was resuspended in 5 ml of PBS under anaerobic conditions, vortexed for 3 min and allowed to settle by gravity for 2 min. Transplant into recipient mice were achieved by gavage with 200 µl of the supernatant and maintained on standard normal-chow diet and water throughout the experiment. All animal studies were approved by the Weizmann Institute of Science Institutional Animal Care and Usage committee (IACUC), application numbers 08680114-3 and 00550113-3; all animal experiments involving transfer of human microbiota into mice were approved by the Weizmann Institute of Science Bioethics and Embrionic Stem Cell Research oversight (ESCRO) committee.

Artificial and caloric sweeteners. The following commercially available NAS were dissolved in mice drinking water to obtain a 10% solution: Sucrazit (5% saccharin, 95% glucose), Sucralite (5% Sucralose), Sweet'n Low Gold (4% Aspartame). 10% glucose (J. T. Baker) and 10% sucrose (Sigma Aldrich) solutions were used for controls. The administered doses of 10% commercial NAS dissolved in water were well below their reported toxic dose (6.3 g per kg (body weight)[27], 16 g per kg (body weight)[28], and 4 g per kg (body weight)[29], for saccharin, sucralose and aspartame, respectively. For experiments conducted with pure saccharin (Sigma Aldrich) a $0.1\,mg\,ml^{-1}$ solution was used in order to meet with FDA defined ADI for saccharin in humans (5 mg per kg (body weight)), according to the following calculation:

$$\frac{\text{ADI } 5mg\,kg^{-1}\,day^{-1} \times \text{average mouse weight } 0.03\,kg}{\text{Average daily liquid intake } 2\,ml} =$$

$$0.075\,mg\,ml^{-1} \longrightarrow 0.1\,mg\,ml^{-1}$$

Glucose and insulin tolerance tests. Mice were fasted for 6 h during the light phase, with free access to water. In all groups of mice where the drinking regime was other than water, it was substituted for water for the period of the fasting and glucose or insulin tolerance test. Blood from the tail vein was used to measure glucose levels using a glucometer (Bayer) immediately before and 15, 30, 60, 90 and 120 min after oral feeding with 40 mg glucose (J. T. Baker) or intra-peritoneal injection with 0.1 U per kg (body weight) Insulin (Biological Industries). Plasma fasting insulin levels were measured in sera collected immediately before the start of GTT using ELISA (Ultra Sensitive Mouse Insulin ELISA Kit, Crystal Chem).

Metabolic studies. Food and drink intake and energy expenditure were measured using the PhenoMaster system (TSE-Systems, Bad Homburg, Germany), which consists of a combination of sensitive feeding sensors for automated measurement and a photobeam-based activity monitoring system detects and records ambulatory movements, including rearing and climbing, in each cage. All parameters were measured continuously and simultaneously. Mice were trained singly-housed in identical cages before data acquisition. To calculate total caloric intake, the following values were used: Chow $3\,kcal\,g^{-1}$, sucrose $0.3938\,kcal\,ml^{-1}$, glucose $0.4\,kcal\,ml^{-1}$, saccharin $0.38\,kcal\,ml^{-1}$, sucralose $0.392\,kcal\,ml^{-1}$ and aspartame $0.38\,kcal\,ml^{-1}$.

***In vitro* anaerobic culturing.** Pooled faecal matter from naive adult WT C57Bl/6 male mice was resuspended in 5 ml PBS in an anaerobic chamber (Coy Laboratory Products, 75% N_2, 20% CO_2, 5% H_2), vortexed for 3 min and allowed to settle by gravity for 2 min. 500 ml of the supernatant were added to a tube containing Chopped Meat Carbohydrate Broth, PR II (BD) and 500 ml of a $5\,mg\,ml^{-1}$ saccharin solution or an equal volume of PBS. Every 3 days, 500 ml of culture were diluted to fresh medium containing saccharin or PBS. After 9 days, cultures were used for inoculation of germ-free mice.

Taxonomic microbiota analysis. Frozen faecal samples were processed for DNA isolation using the MoBio PowerSoil kit according to the manufacturer's instructions. 1 ng of the purified faecal DNA was used for PCR amplification and sequencing of the bacterial 16S rRNA gene. ~365bp Amplicons spanning the variable region 2 (V2) of the 16S rRNA gene were generated by using the following barcoded primers: Fwd 5′-AGAGTTTGATCCTGGCTCAG-3′, Rev 5′-TGCTGCCTCCCGTAGG AGT-3′. The reactions were subsequently pooled in an equimolar ratio, purified (PCR clean kit, Promega), and used for Illumina MiSeq sequencing to a depth of at least 18,000 reads per sample (mean reads per sample 139,148 ± 5264 (s.e.m.)).

Reads were then processed using the QIIME (quantitative insights into microbial ecology) analysis pipeline as described[30,31], version 1.8. Paired-end joined sequences were grouped into operational taxonomic units (OTUs) using the UCLUST algorithm and the GreenGenes database[32]. Sequences with distance-based similarity of 97% or greater over median sequence length of 353 bp were assigned to the same OTU. Samples were grouped according to the treatment. Analysis was performed at each taxonomical level (phylum, genus and OTU level) separately. For each taxon, G test was performed between the different groups. P values were FDR-corrected for multiple hypothesis testing.

Shotgun pyrosequencing and sequence mapping. This was performed as previously described[33], with the following modifications: 1 µg of DNA was sheared using the Covaris 5200 system (Covaris, Inc., Woburn, MA, USA), followed by end repair, ligation to adapters, an 8-cycle PCR amplification (Kappa HiFi) and sequenced using an Illumina HiSeq to a minimal depth of 11,773,345 reads per sample (mean reads per sample 20,296,086 ± 637,379 (s.e.m.), read length 51 bp). Illumina sequence reads were mapped to the human microbiome reference genome database of the Human Microbiome Project (http://hmpdacc.org/HMREFG/, ref. 16), and to a gut microbial gene catalogue[34] using GEM mapper[35] with the following parameters:

$$\text{-m } 3 \text{ –s } 0 \text{ –q offset-33 –gem-quality-threshold } 26$$

Microbial species abundance was measured as the fraction of reads that mapped to a single species in the database. An expectation–maximization (EM) algorithm adapted from Pathoscope[36] was employed to determine the correct assignment of reads that mapped to more than one species. We considered only species for which at least 10% of the genome was covered (each coverage bin was 10,000-bp long) in at least one of the growth conditions (saccharin, water, or glucose). Reads mapped to the gut microbial gene catalogue were assigned a KEGG ID according to the mapping available with the catalogue. Genes were subsequently mapped to KEGG pathways, and only pathways whose gene coverage was above 0.2 were included. To calculate the contribution of different bacteria to the overrepresentation of glycan degradation pathways, reads that were mapped to genes in the gut microbial gene catalogue that belong to glycan degrading pathways were extracted and re-mapped the HMP reference genome database, seeking germs that had the highest contribution.

Short chain fatty acid quantification. To determine the level of free fatty acids analytic HPLC (Agilent 1260) was performed as described previously[37]. In brief, standard solutions of acetate, butyrate and propionate (all from Sigma-Aldrich) were prepared at various concentrations (0.01–0.2 M). These solutions were analysed using HPLC, successive with quadrupole time-of-flight mass spectrometry with a step-gradient of solvent solution from 0% to 60% of CH_3CN with 0.1% formic acid to obtain calibration curve for each fatty acid. Faecal media samples were dissolved with 0.1% formic acid and analysed in a similar manner to measure the total concentration of all three free fatty acids.

Analysis of the relationship between NAS consumption and clinical parameters in humans. All human studies were approved by the Tel Aviv Sourasky Medical Center Institutional Review Board, approval number TLV-0658-12, TLV-0050-13 and TLV-0522-10; Kfar Shaul Hospital Institutional Review Board, approval number 0-73; and the Weizmann Institute of Science Bioethics and Embrionic Stem Cell Research oversight (ESCRO) committee. The trial was reported to http://clinicaltrials.gov/, identifier NCT01892956. The study did not necessitate or involve randomization. For each individual in the clinical nutritional study, after signing an informed consent, multiple parameters were collected including BMI, body circumferences, fasting glucose levels, general questionnaire, complete blood counts and general chemistry parameters, a validated long-term food frequency questionnaire[38–40].

Long-term NAS consumption was quantified directly from answers to an explicit question regarding artificial sweeteners that participants filled out in their food frequency questionnaire. We then used the Spearman correlation to examine the relationship between NAS consumption and each of the above parameters, and FDR corrected for the multiple hypotheses tests performed.

Statistics. The following statistical analyses were used: in GTT, a two-way ANOVA and Bonferroni post-hoc analysis were used to compare between groups in different time-points, and one-way ANOVA and Tukey post hoc analysis or unpaired two-sided Student t-test were used to compare between AUC of multiple or two groups, respectively. Bartlett's or F-test for equal variance were employed and no significant difference was observed between variances of the compared groups. For comparison of taxonomic data, a G-test was used and P values were FDR-corrected for multiple hypothesis testing. In metagenomics and clinical and taxonomic data from humans, Pearson and Spearman were used for correlation tests, and Mann–Whitney U was used to compare clinical parameters between groups. $P < 0.05$ was considered

significant in all analyses (* denotes $P < 0.05$, **$P < 0.01$, ***$P < 0.001$). In all relevant panels, symbols or horizontal lines represent the mean, and error bars represent s.e.m. For mouse experiments, cohort sizes match common practice of the described experiments. For human experiments, sample size was chosen to validate statistical analyses. No mice or data points were excluded from analyses. In the human studies, all humans older than 18 years of age who enrolled were included. Exclusion criteria included pregnancy.

27. Taylor, J. D., Richards, R. K. & Wiegand, R. G. Toxicological studies with sodium cyclamate and saccharin. *Food Cosmet. Toxicol.* **6,** 313–327 (1968).
28. Goldsmith, L. A. Acute and subchronic toxicity of sucralose. *Food Chem. Toxicol.* **38** (Suppl. 2), 53–69 (2000).
29. Magnuson, B. A. *et al.* Aspartame: a safety evaluation based on current use levels, regulations, and toxicological and epidemiological studies. *Crit. Rev. Toxicol.* **37,** 629–727 (2007).
30. Caporaso, J. G. *et al.* QIIME allows analysis of high-throughput community sequencing data. *Nature Methods* **7,** 335–336 (2010).
31. Elinav, E. *et al.* NLRP6 inflammasome regulates colonic microbial ecology and risk for colitis. *Cell* **145,** 745–757 (2011).
32. DeSantis, T. Z. *et al.* Greengenes, a chimera-checked 16S rRNA gene database and workbench compatible with ARB. *Appl. Environ. Microbiol.* **72,** 5069–5072 (2006).
33. Blecher-Gonen, R. *et al.* High-throughput chromatin immunoprecipitation for genome-wide mapping of *in vivo* protein–DNA interactions and epigenomic states. *Nature Protocols* **8,** 539–554 (2013).
34. Qin, J. *et al.* A human gut microbial gene catalogue established by metagenomic sequencing. *Nature* **464,** 59–65 (2010).
35. Marco-Sola, S., Sammeth, M., Guigó, R. & Ribeca, P. The GEM mapper: fast, accurate and versatile alignment by filtration. *Nature Methods* **9,** 1185–1188 (2012).
36. Francis, O. E. *et al.* Pathoscope: species identification and strain attribution with unassembled sequencing data. *Genome Res.* **23,** 1721–1729 (2013).
37. Kolodkin-Gal, I. *et al.* D-amino acids trigger biofilm disassembly. *Science* **328,** 627–629 (2010).
38. Shahar, D., Fraser, D., Shai, I. & Vardi, H. Development of a food frequency questionnaire (FFQ) for an elderly population based on a population survey. *J. Nutr.* **133,** 3625–3629 (2003).
39. Shahar, D., Shai, I., Vardi, H., Brener-Azrad, A. & Fraser, D. Development of a semi-quantitative Food Frequency Questionnaire (FFQ) to assess dietary intake of multiethnic populations. *Eur. J. Epidemiol.* **18,** 855–861 (2003).
40. Shai, I. *et al.* Dietary evaluation and attenuation of relative risk: multiple comparisons between blood and urinary biomarkers, food frequency, and 24-hour recall questionnaires: the DEARR study. *J. Nutr.* **135,** 573–579 (2005).
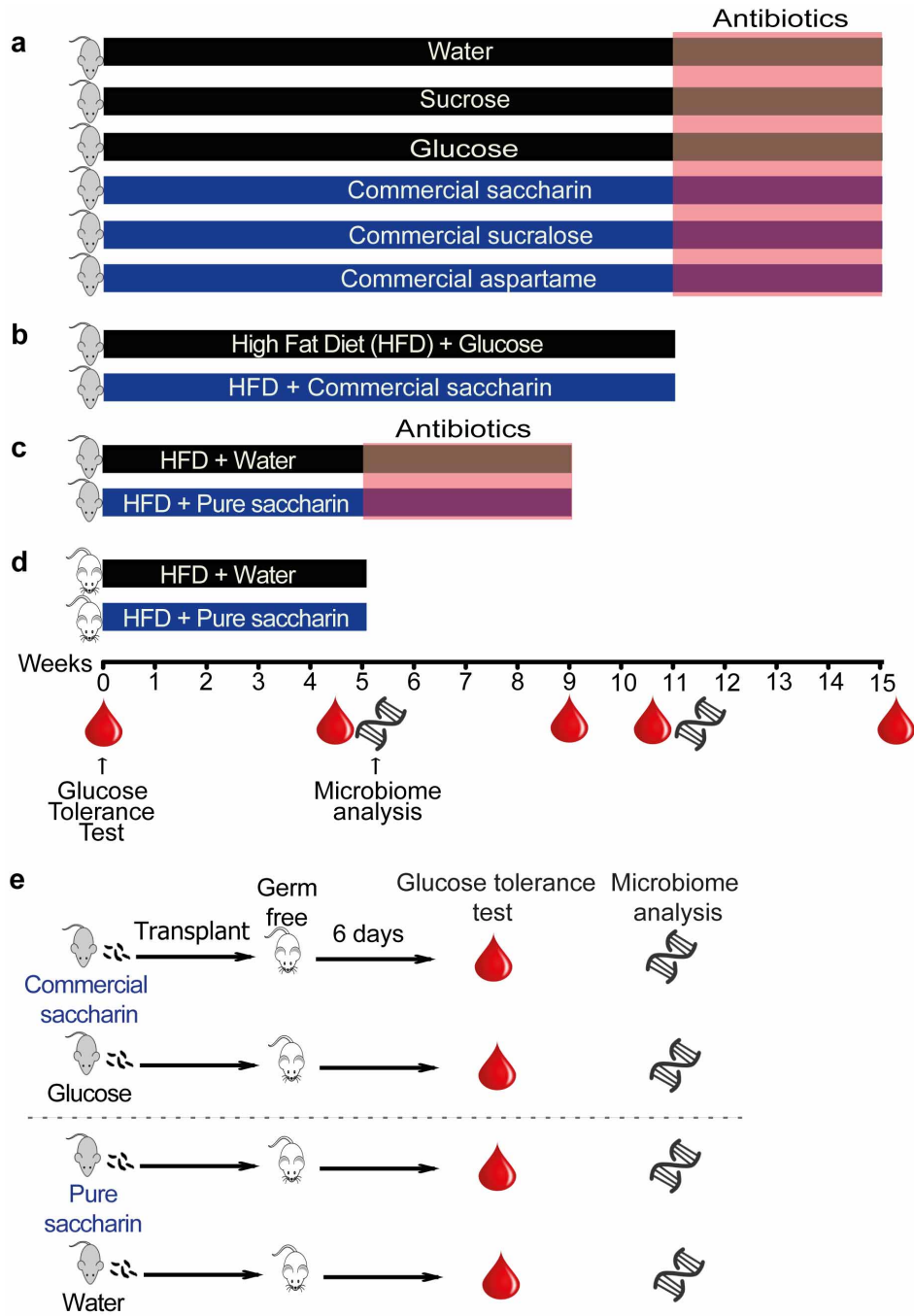
Extended Data Figure 1 | Experimental scheme. 10-week-old C57Bl/6 male mice were treated with the following dietary regimes. **a**, Drinking commercially available non-caloric artificial sweeteners (NAS; saccharin, sucralose and aspartame) or glucose, sucrose or water as controls and fed a normal-chow (NC) diet. **b**, Drinking commercially available saccharin or glucose as control and fed a high-fat diet (HFD). **c**, Drinking pure saccharin or water and fed HFD. **d**, As in **c**, but with outbred Swiss-Webster mice. Glucose tolerance tests, microbiome analysis and supplementation of drinking water with antibiotics were performed on the indicated time points. **e**, Schematic of faecal transplant experiments.
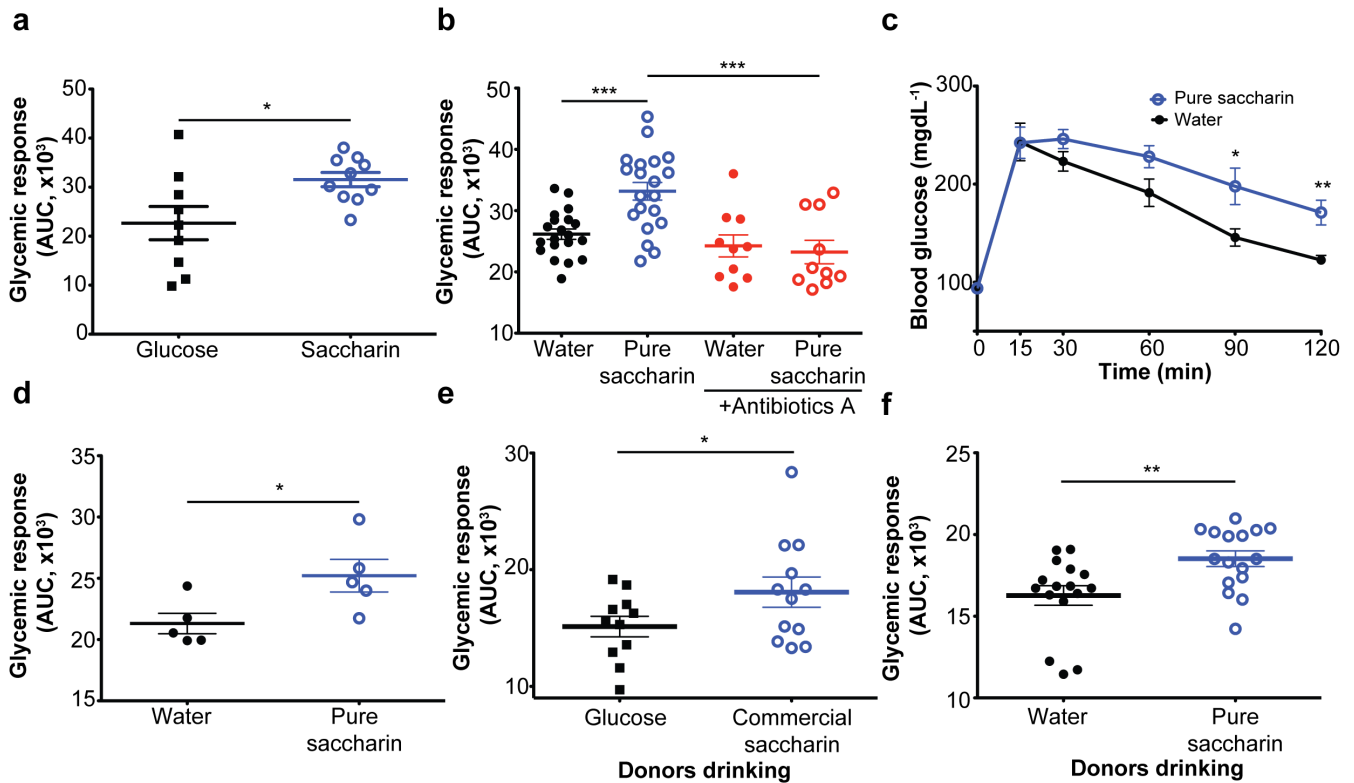
Extended Data Figure 2 | Artificial sweeteners induce glucose intolerance. **a**, AUC of mice fed HFD and commercial saccharin ($N = 10$) or glucose ($N = 9$). **b**, AUC of HFD-fed mice drinking $0.1\,\mathrm{mg\,ml^{-1}}$ saccharin or water for 5 weeks ($N = 20$), followed by 'antibiotics A' ($N = 10$). **c, d**, OGTT and AUC of HFD-fed outbred Swiss-Webster mice ($N = 5$) drinking pure saccharin or water. **e, f**, Faecal samples were transferred from donor mice ($N = 10$) drinking commercially available, pure saccharin, glucose or water controls into 8-week-old male Swiss-Webster germ-free recipient mice. AUC of germ-free mice 6 days following transplant of microbiota from commercial saccharin- ($N = 12$) and glucose-fed mice ($N = 11$) (**e**); or pure saccharin- ($N = 16$) and water-fed ($N = 16$) donors (**f**). Symbols (GTT) or horizontal lines (AUC), means; error bars, s.e.m. *$P < 0.05$, **$P < 0.01$, ***$P < 0.001$, ANOVA and Tukey post hoc analysis (GTT) or unpaired two-sided Student t-test (AUC). Each experiment was repeated twice.
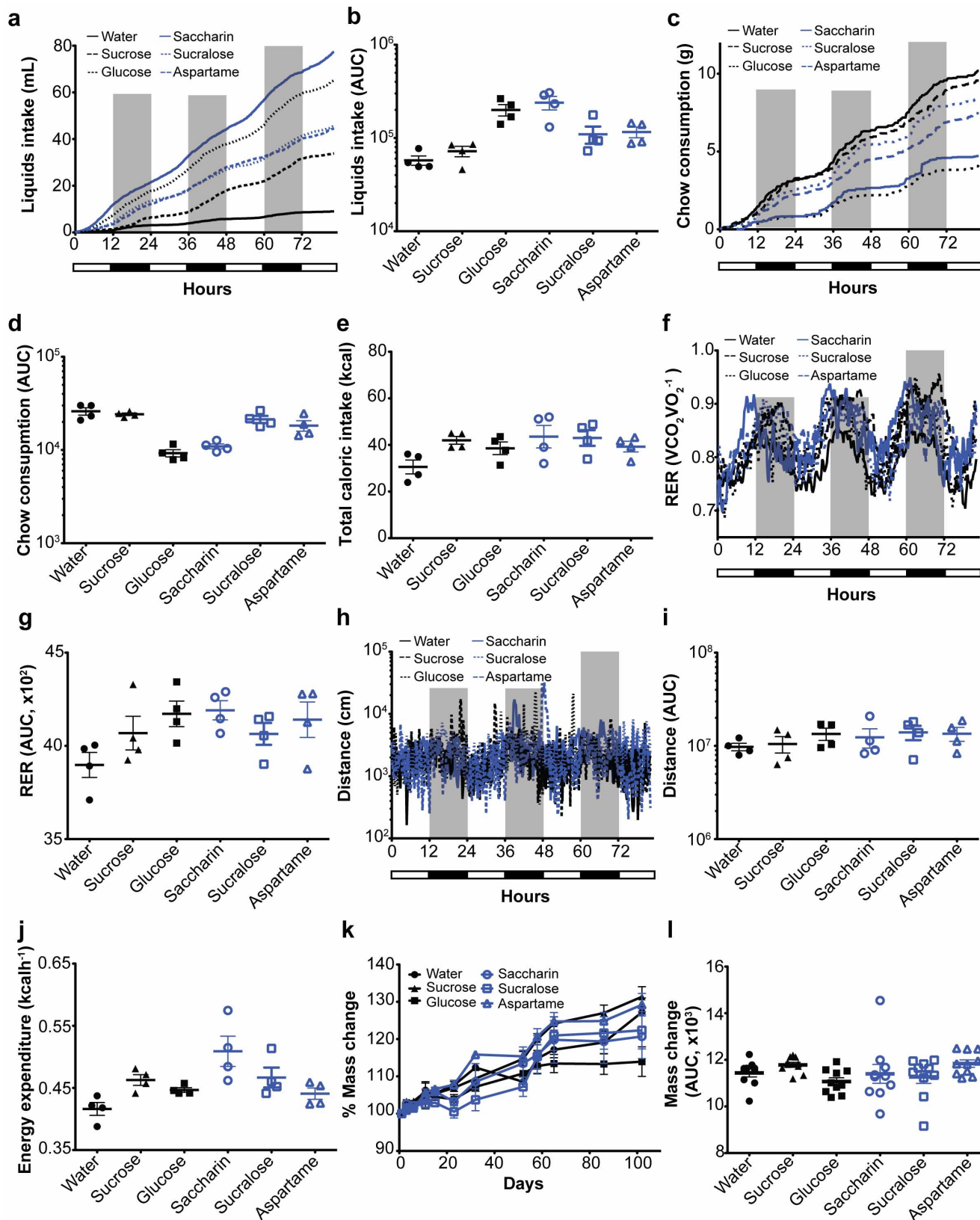
Extended Data Figure 3 | Metabolic characterization of mice consuming commercial NAS formulations. 10-week-old C57Bl/6 mice ($N = 4$) were given commercially available artificial sweeteners (saccharin, sucralose and aspartame) or controls (water, sucrose or glucose, $N = 4$ in each group) and fed normal-chow diet. After 11 weeks, metabolic parameters were characterized using the PhenoMaster metabolic cages system for 80 h. Light and dark phases are denoted by white and black rectangles on the x-axis, respectively, and grey bars for the dark phase. **a**, Liquids intake. **b**, AUC of **a**. **c**, Chow consumption. **d**, AUC of **c**. **e**, Total caloric intake from chow and liquid during 72 h (see methods for calculation). **f**, Respiratory exchange rate (RER). **g**, AUC of **f**. **h**, Physical activity as distance. **i**, AUC of **h**. **j**, Energy expenditure. **k**, Mass change compared to original mouse weight during 15 weeks ($N = 10$). **l**, AUC of **k**. The metabolic cages characterization and weight-gain monitoring were repeated twice.
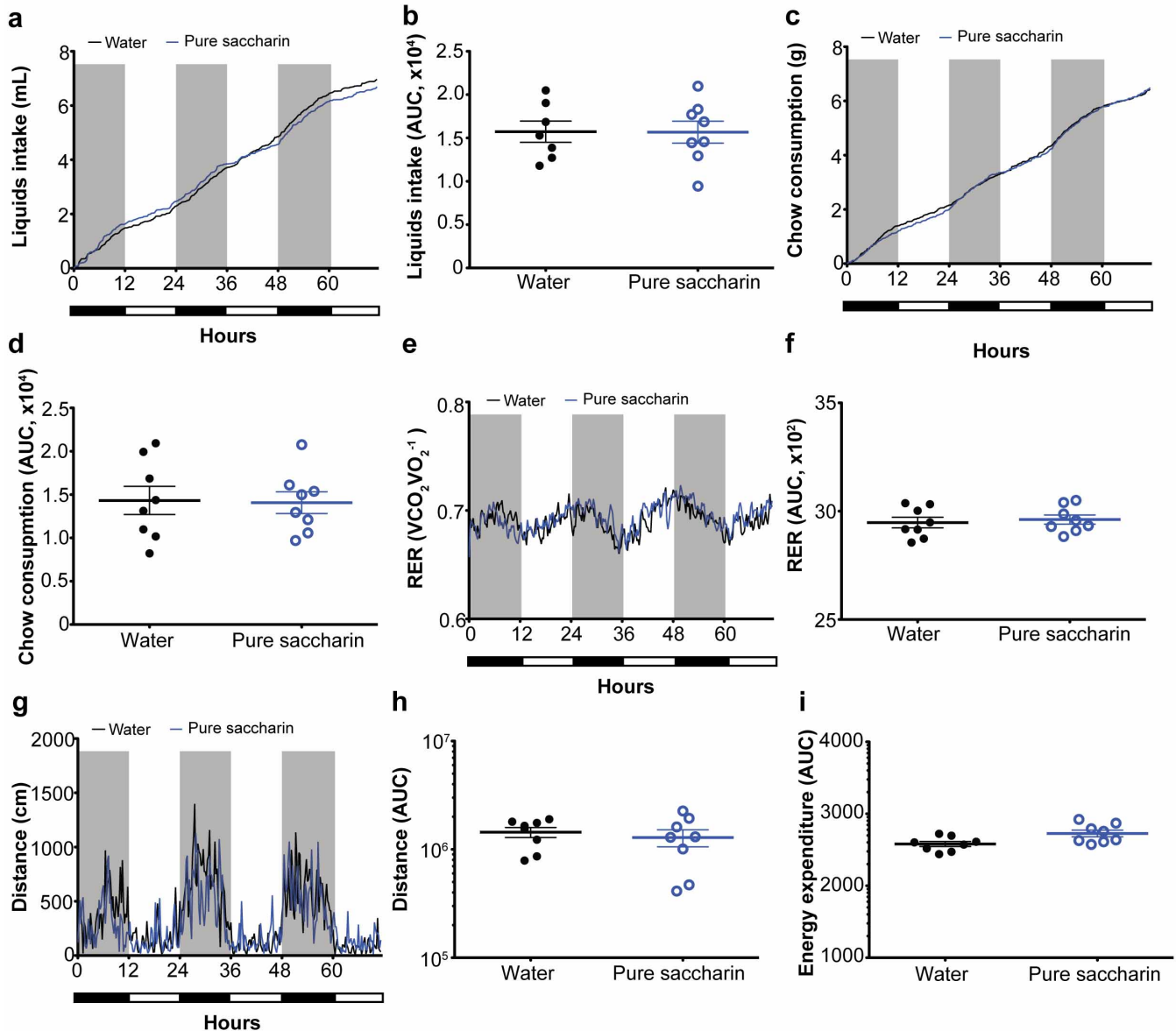
Extended Data Figure 4 | Metabolic characterization of mice consuming HFD and pure saccharin or water. 10-week-old C57Bl/6 mice ($N = 8$) were fed HFD, with or without supplementing drinking water with 0.1 mg ml^{-1} pure saccharin. After 5 weeks, metabolic parameters were characterized using the PhenoMaster metabolic cages system for 70 h. Light and dark phases are denoted by white and black rectangles on the x-axis, respectively, and grey bars for the dark phase. **a**, Liquids intake. **b**, AUC of **a**. **c**, Chow consumption. **d**, AUC of **c**. **e**, Respiratory exchange rate (RER). **f**, AUC of **e**. **g**, Physical activity as distance. **h**, AUC of **g**. **i**, Energy expenditure. The metabolic cages characterization was repeated twice.
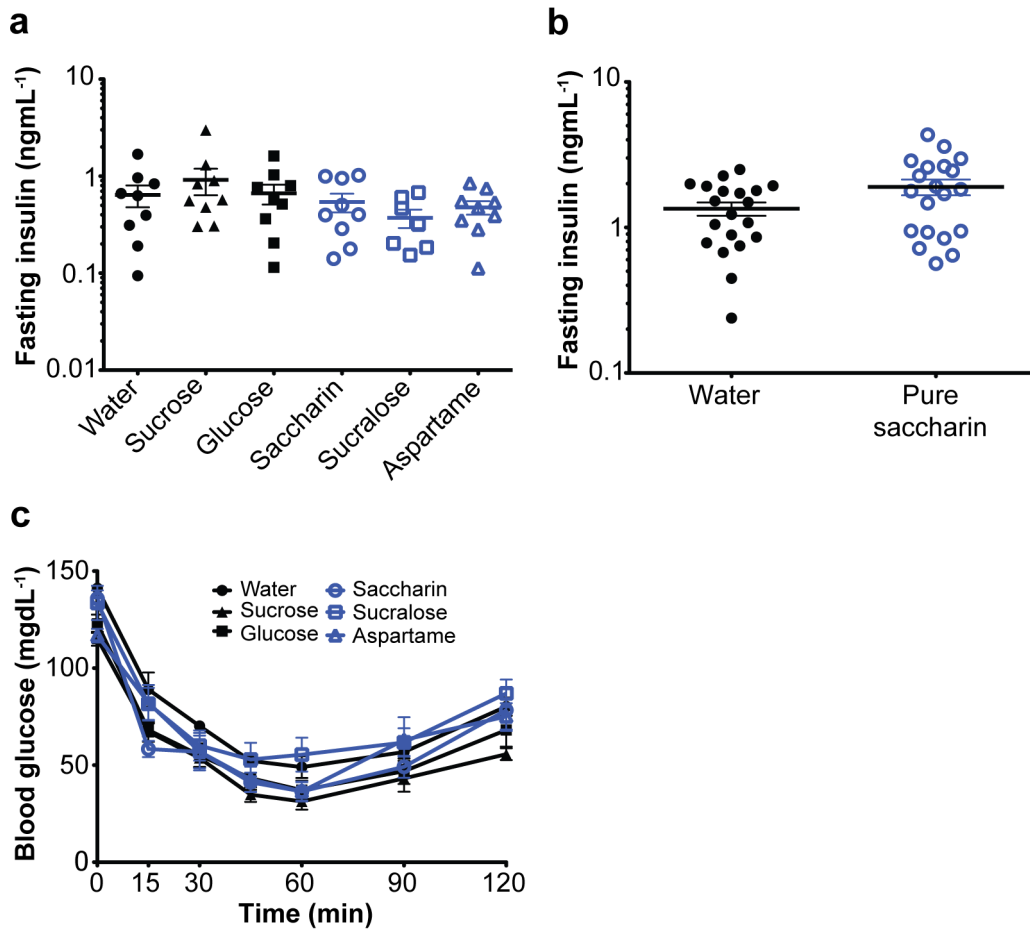
Extended Data Figure 5 | Glucose intolerant NAS-drinking mice display normal insulin levels and tolerance. a, Fasting plasma insulin measured after 11 weeks of commercial NAS or controls ($N = 10$). **b**, Same as **a**, but measured after 5 weeks of HFD and pure saccharin or water ($N = 20$). **c**, Insulin tolerance test performed after 12 weeks of commercial NAS or controls ($N = 10$). Horizontal lines (**a**, **b**) or symbols (**c**) represent means; error bars, s.e.m. All measurements were performed on two independent cohorts.
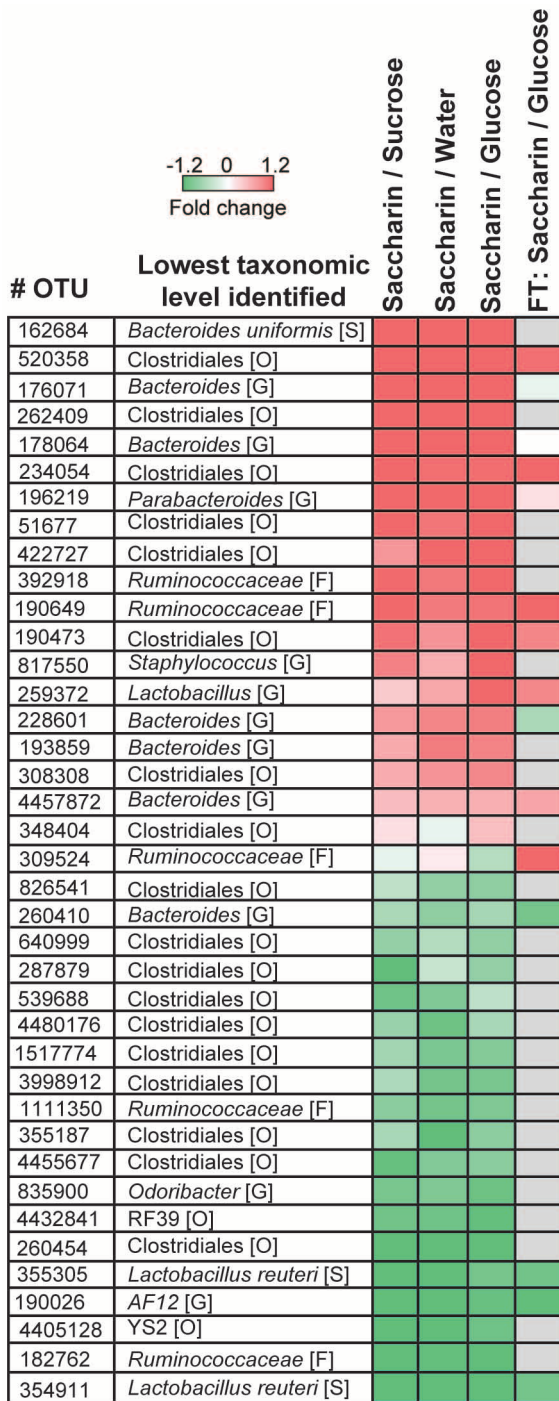
Extended Data Figure 6 | Dysbiosis in saccharin-consuming mice and germ-free recipients. Heat map representing W11 logarithmic-scale fold taxonomic differences between commercial saccharin and water or caloric sweetener consumers ($N = 5$ in each group). Right column, taxonomical differences in germ-free mice following faecal transplantation from commercial saccharin- (recipients $N = 15$) or glucose-consuming mice ($N = 13$). OTU number (GreenGenes) and the lowest taxonomic level identified are denoted.

a *Bacteroides vulgatus*

Abundance (×10⁻⁴, per 10kb bins)

Saccharin Glucose Water

Week 0
Week 11

b *Akkermansia muciniphila*

Abundance (×10⁻⁴, per 10kb bins)

Week 0
Week 11

Saccharin Glucose Water

c

Substrate	Module	Product	Glucose (W11/W0)	Saccharin (W11/W0)	GF transplanted with treated culture (Sac/PBS)
Glucose	PtsG | Crr	Glucose 6-phosphate			
N-Acetyl-D-glucosamine	NagE	N-Acetyl-D-glucosamine 6-phosphate			
Maltose	MalX | Crr	Maltose 6-phosphate			
D-glucosamine	GamP	D-glucosamine 6-phosphate			
Sucrose	ScrA	Sucrose-6-phosphate			
β-glucosides	BglF	Phospho-β-glucoside			
Arbutin / Salicin	AscF | Crr	Arbutin 6-phosphate / Salicin 6-phosphate			
Trehalose	TreB | Crr	Trehalose 6-phosphate			
N-Acetyl-muramic acid	MurP | Crr	N-Acetylmuramic acid 6-phosphate			

-0.5 0 1
Fold change

d

| KEGG ID	Pathway	Saccharin (W11/W0)	HFD pure sac / water
ko01053	Biosynthesis of siderophore group nonribosomal peptides		
ko02040	Flagellar assembly		
ko00643	Styrene degradation		
ko00053	Ascorbate and aldarate metabolism		
ko00633	Nitrotoluene degradation		
ko05111	Vibrio cholerae pathogenic cycle		
ko00930	Caprolactam degradation		
ko00380	Tryptophan metabolism		
ko00565	Ether lipid metabolism		
ko00410	beta-Alanine metabolism		
ko00281	Geraniol degradation		
ko00791	Atrazine degradation		
ko02030	Bacterial chemotaxis		
ko00440	Phosphonate and phosphinate metabolism		
ko00540	Lipopolysaccharide biosynthesis		

-0.2 1 0.3
Fold change
(Week 11 / Week 0)

Extended Data Figure 7 | Functional analysis of saccharin-modulated microbiota. a, b, Changes in bacterial relative abundance occur throughout the bacterial genome. Shown are changes in sequencing coverage along 10,000 bp genomic regions of *Bacteroides vulgatus* (**a**) and *Akkermansia muciniphila* (**b**), with bins ordered by abundance in week 0 of saccharin-treated mice. **c,** Fold change in relative abundance of modules belonging to phosphotransferase systems (PTS) between week 11 and week 0 in mice drinking commercial saccharin, glucose or water. Module diagram source: KEGG database. **d,** Enriched KEGG pathways (fold change > 1.38 as cutoff) in mice consuming HFD and pure saccharin versus water compared to the fold change in relative abundance of the same pathways in mice consuming commercial saccharin (week 11/week 0).
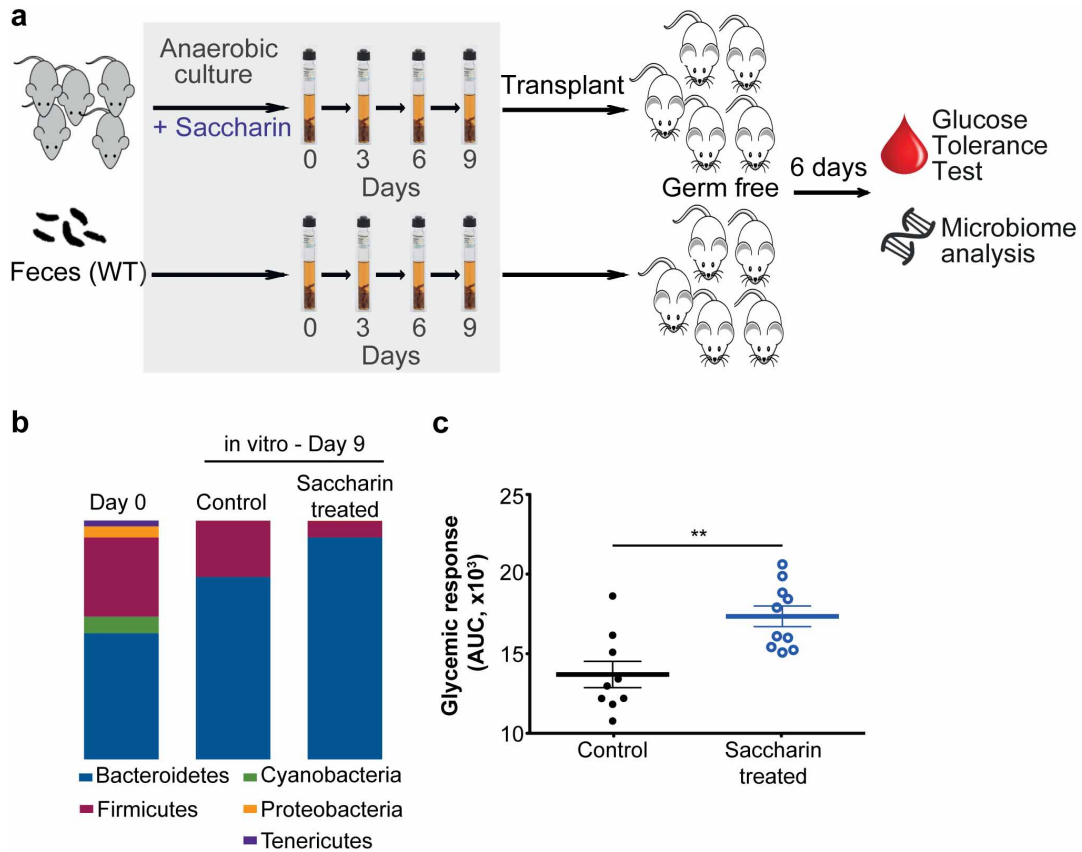
Extended Data Figure 8 | Saccharin directly modulates the microbiota.
a, Experimental schematic. **b**, Relative taxonomic abundance of anaerobically cultured microbiota. **c**, AUC of germ-free mice 6 days following transplantation with saccharin-enriched or control faecal cultures ($N = 10$ and $N = 9$, respectively). Horizontal lines, means; error bars, s.e.m. **$P < 0.01$, unpaired two-sided Student t-test. The experiment was repeated twice.
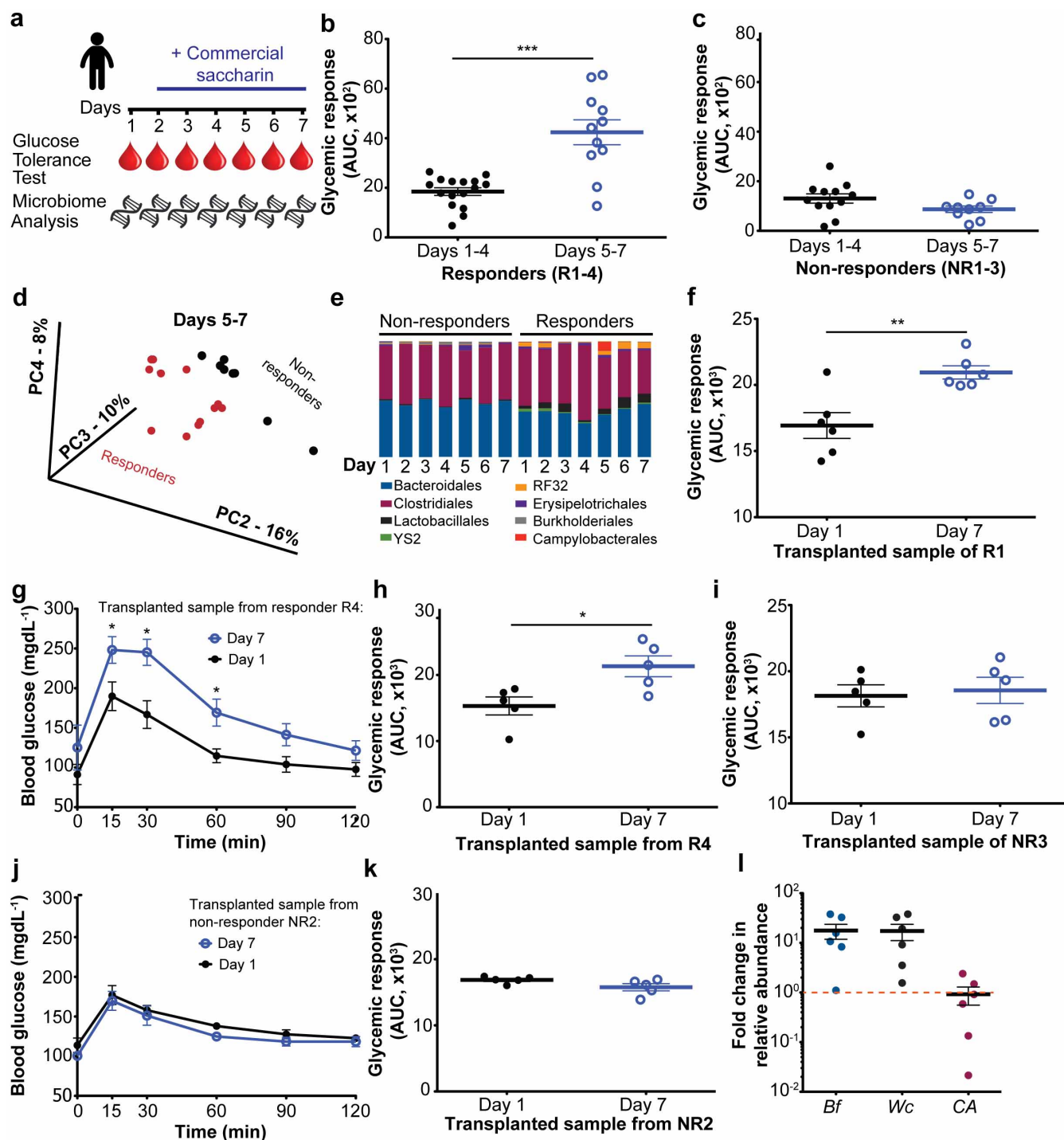
Extended Data Figure 9 | Impaired glycaemic control associated with acute saccharin consumption in humans is transferable to germ-free mice.
a, Experimental schematic ($N = 7$). **b, c**, Daily incremental AUC of days 1–4 versus days 5–7 in four responders (**b**) or three non-responders (**c**). **d**, Principal coordinates analysis (PCoA) of weighted UniFrac distances of 16S rRNA sequences demonstrating separation on principal coordinates 2 (PC2), 3 (PC3) and 4 (PC4) of microbiota from responders (N samples = 12) versus non-responders ($N = 8$) during days 5–7. **e**, Order-level relative abundance of taxa samples from days 1–7 of responders and non-responders. **f**, AUC in germ-free mice ($N = 6$) 6 days following faecal transplantation from samples of responder 1 (R1) collected before and after 7 days of saccharin consumption. **g, h**, OGTT and AUC in germ-free mice ($N = 5$) 6 days after receiving faecal samples collected from responder 4 (R4) before and after 7 days of saccharin consumption. **i**, AUC in germ-free mice ($N = 5$) 6 days following faecal transplantation from samples of non-responder 3 (NR3) collected before and after 7 days of saccharin consumption. **j, k**, OGTT and AUC in germ-free mice ($N = 5$) 6 days after receiving faecal samples collected from non-responder 2 (NR2) before and after 7 days of saccharin consumption. **l**, Fold taxonomical abundance changes of selected OTUs, altered in germ-free recipients of D7 versus D1 microbiomes from R1. Dot colour same as in **e**, bacterial orders. Symbols (GTT) or horizontal lines (AUC), means; error bars, s.e.m. *$P < 0.05$, **$P < 0.01$, ***$P < 0.001$, two-way ANOVA and Bonferroni post-hoc analysis (GTT), unpaired two-sided Student t-test (AUC).